

A DIRECT DISCRETE-TIME REDUCED ORDER ROBUST MODEL REFERENCE ADAPTIVE CONTROL FOR GRID-TIED POWER CONVERTERS WITH LCL FILTER

Paulo J. D. O. Evald^{1,2}, Rodrigo V. Tambara¹, Hilton A. Gründling¹

¹Universidade Federal de Santa Maria (UFSM), Santa Maria – RS, Brazil

²Universidade Franciscana (UFN), Santa Maria – RS, Brazil

e-mail: paulo.evald@gmail.com, rodvarella@yahoo.com.br, ghilton03@gmail.com

Abstract – In this work is presented the design of a direct discrete-time reduced order RMRAC (Robust Model Reference Adaptive Control) applied to the grid-side current control of a static grid-tied voltage-fed 3-wire converter with LCL filter. The proposed controller tracks the reference model output as close as a higher order RMRAC, with similar performance. Furthermore, it rejects exogenous disturbances from grid without the need of conventional resonant controllers, often employed in this kind of application. To design the reduced order controller, the LCL filter is approximated to a first order transfer function, neglecting the capacitor influence. Besides, it is shown mathematically that capacitor is the main element that compounds the additive dynamics, which is considered as unmodelled dynamics to design the controller. Furthermore, experimental results performed in a TMS320F28335 Delfino microcontroller are presented and show the similarity of performance between proposed control method and higher order RMRAC, regarding to harmonics content, which indicate its feasibility.

Keywords – Computational Burden Reduction, Controller Order Reduction, Grid-tied Converters, LCL Filter, Robust Adaptive Control.

I. INTRODUCTION

Distributed power generation systems based on renewable energy sources are fast growing worldwide in the last years [1], once electrical generation remains very intense. To contribute to this continuous expansion, thermal power stations utilise fossil matter that generates pollution and show no tendency to reduce energy production costs [2], while renewable energy is essentially unlimited and environmentally sustainable [3].

In these renewable energy applications, modulated voltage-source converters have been more and more used [4]. To realise connection of static power converters to the electrical grid, L or LCL filters are commonly used [5], because voltage-fed converters modulated by PWM (*Pulse Width Modulation*) present high harmonic contents of voltage at their outputs, which are reflected in the current. Therefore, to keep the current harmonics from commutations below standard levels, the converters are connected to the grid through filters [6], generally L or LCL filters. Between the two most popular filters, LCL filter has some advantages over L

filter, such as higher harmonic attenuation [7]–[9], which is -60dB/dec , while L filter attenuates only -20dB/dec . In addition, although the LCL filter has a more complex topology compared to the L filter, LCL filter is built with smaller reactive elements, which results in a lower cost, weight, switching frequency and reactive power consumption in the grid fundamental frequency [10], [11]. Thus, in this work, an LCL filter is used as interface between converter and the grid.

However, high resonance peaks in the LCL filter at uncertain frequencies may turn the current control loop unstable [7], consequently reducing the grid power quality [12]. There are techniques in the literature to dampen this resonance peak using passive or active damping. The first method is dependent on the grid characteristics at PCC (Point of Common Coupling), which in high powers entails high cost of energy. In this method, a resistor is connected in series with the filter capacitor, which dampens current oscillations. However, this method increases power losses and decreases high order harmonics attenuation [13]. By the other hand, the active damping methods are based on the application of a controller, without adding any external passive components. In the literature, there are several approaches to control grid-side currents of LCL filter, including: PI (Proportional-Integral) [10], [14], [15], PI with Resonant Controller [12], [16], Multi-resonant Control [17], Optimal Control [18], [19], Robust Control [20]–[23], Sliding Mode Control [24], [25], Predictive Control [26], among others.

Even based on fixed gain controllers, these approaches demonstrate good results. However, it is noteworthy that LCL filter inductance, converter side and mainly grid side, may vary due to the influence of magnetic permeability of the core, which is a function of converter-side current magnitude and due to the short circuit power in the PCC, respectively [27]. Therefore, fixed gain controllers do not guarantee good performance against unmodelled dynamics or parametric variations outside the projected operating range, because their stability margin are not very high and their harmonic suppression abilities are limited. At this point, robust adaptive controllers stand out advantageously over fixed gain controllers, because their gains are adjusted online, what makes them suitable for treating plants with uncertain parameters, such as grid-tied converters with LCL filters, where the line impedance is unknown. In the literature, there are works that mitigate LCL filter resonance with robust adaptive controllers, such as: [9], [27]–[34].

In the works [9], [29] are presented third-order discrete-time RMRAC (Robust Model Reference Adaptive Control) based

Manuscript received 07/06/2020; first revision 08/27/2020; accepted for publication 09/08/2020, by recommendation of Editor Demercil de Souza Oliveira Jr. <http://dx.doi.org/10.18618/REP.2020.3.0039>

on modified RLS (Recursive Least Squares) algorithms. In these works experimental results proved the good performance of adaptive controllers dealing with grid-tied converters by LCL filter. In these works, controllers reject exogenous disturbance without conventional Resonant Controllers and tracked model reference output very closely. On the other hand, in [30], a multi-loop control is proposed for grid-side currents control. The controller is composed by a discrete-time MRAC (Model Reference Adaptive Control) with Gradient algorithm as outer loop for compensation of disturbances and compare two control strategy (a Proportional plus Derivative and a Proportional controller) based on capacitor voltage or capacitor current feedback for inner loop, designed for reference tracking. By means of simulations, authors shown that capacitor current feedback-based controller presented more robustness than capacitor voltage feedback-based controller. In other approach, in [32], a system sensitivity based-control strategy was proposed. In this work, authors developed a new adaptive current control strategy that involves the elimination of sensitivity error and can be suitable for different control systems, although only simulation results were presented to validate the proposed approach. Next, in [34], an Adaptive Notch Filter-based PI control was proposed to deal with LCL resonance peaks. Again, simulation results were presented to validate control system and demonstrated good results with mitigation of the LCL filter resonance that leads to a high quality current injection into the electrical grid. Differently from aforementioned works, in [28], authors proposed to combine a deadbeat controller and an adaptive one to guarantee zero error in steady state on current control. In this research, both controllers work in parallel, maintaining high-speed response typical from deadbeat controllers and adaptability from another. Finally, in [31], [33], authors combined MRAC (Model Reference Adaptive Control) with SMC (Sliding Mode Control), with tracking error as its surface, to obtain new robust adaptive controllers. By means of simulation, exogenous disturbances were properly rejected with these active methods of mitigation.

As an alternative to these works, it is proposed a lower computational burden direct discrete-time RMRAC approach by reduction of its order that reduces significantly the time processing of control algorithm, simplifies the design and reduces implementation complexity, maintaining similar performance, regarding to harmonics content, which are the main contributions of this paper. To design this reduced order controller, the LCL filter model is approximated to a first order transfer function, neglecting the capacitor influence, which is considered as an additive dynamics. Besides, it is shown mathematically that capacitor is the main dynamics that compounds the additive dynamics. Furthermore, the adaptation law used to adjust controller gains is a Gradient algorithm, which requires significantly less calculation than aforementioned RLS algorithms, due to its simple structure.

Currently, there are a few works in the literature dealing with order reduction of RMRAC applied to grid-tied power converters with LCL filters, such as [27], where a MRAC, without robustness guaranteed and based on a second-order model reference, is presented. Then, in this work is shown through experimental results, that proposed first-order active

damping strategy is suitable for this application and obtain satisfactory results, respecting IEEE 1547 Standard.

For the controller design it will be assumed that the grid is predominantly inductive, which is plausible for high power systems. In addition, it will also be considered that there is only one converter connected to the PCC and that there are no nonlinear loads and effects from capacitive banks, to avoid increase the system order, because the parametric uncertainties and exogenous disturbances present in grid-tied power systems already make the discrete-time control project a nontrivial task [12].

Moreover, it is known that continuous plants with relative degree greater than 2, when discretised by Z transform, have zeros outside of unit circle at Z plane (i.e., discrete-time nonminimum-phase plants) [35]. The LCL filter is typically modelled as a third order plant with relative degree equal to 3, in continuous-time. In contrast to minimum-phase plants, where the effects of zeros can be cancelled with stable poles, nonminimum zeros can not be cancelled inserting unstable poles. In the literature, there are some techniques that deal with nonminimum-phase plants, however these techniques result in more complex control projects due to the increase of new parameters to be designed (see [36]–[38]), for continuous-time applications. In RMRAC strategy it is not different, we cannot cancel the nonminimum-phase zeros inserting poles, as it is made with minimum-phase zeros by means of Model Reference Control theory. Thus, it is necessary to circumvent this problem, maintaining reference tracking, robustness and stability. When approaching the plant to an equivalent reduced order model, the plant nonminimum phase issue is favourably circumvented, by considering only a portion of known part of the plant in the control design. However, it must be taken into account that there will be influence of the unmodelled dynamics on the plant response experimentally, including the neglected dynamics on control design.

The reminder of this paper is structured as follows: Section 2 presents the mathematical model of grid-tied converter with LCL filter and the plant order reduction for reduced order controller design. Following, in Section 3 and 4 are presented the high order direct RMRAC and proposed reduced order RMRAC approach, theory and design, both in discrete-time and with experimental results, respectively. Finally, Section 5 gives the conclusion of this work.

II. GRID-TIED CONVERTER WITH LCL FILTER

The system consists of a primary power source, capacitor bank, converter and LCL filter. The primary power source may be a wind generator, photovoltaic panel or any other form of distributed power generation. In this work, the power source is a continuous voltage source. The capacitor bank is used for the energy accumulation in the form of direct voltage and converter performs the DC-AC (Direct Current to Alternating Current) conversion of the energy stored in the capacitor bank, generating the control voltages, necessary to control of grid-injected currents. Also, a microcontroller is responsible by taking converter voltages and currents, PCC voltage and line voltages measurements and store them, as well as, control law computation and converter switching, here a SVM (Space Vector Modulation) technique.

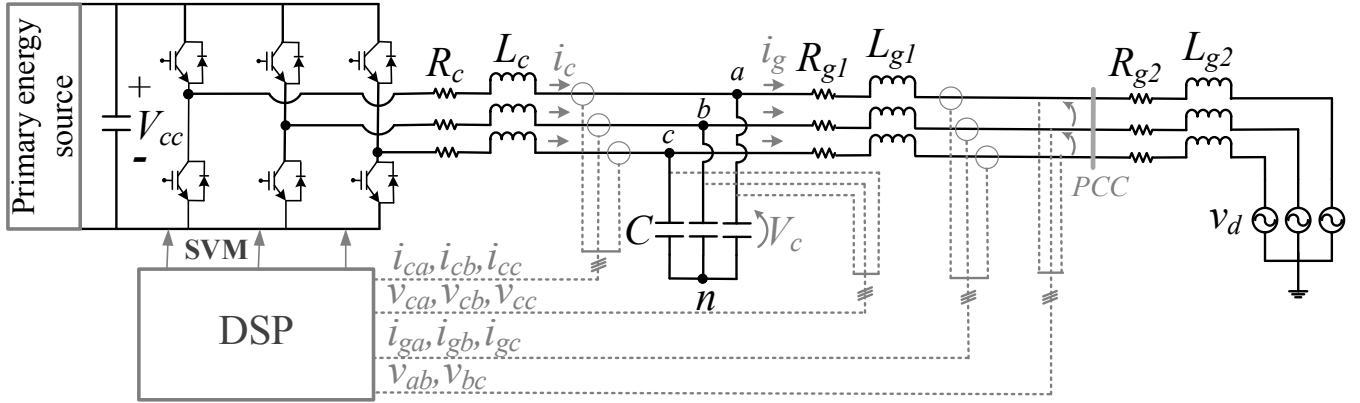


Fig. 1. Grid-tied voltage-fed 3-wire static converter with LCL filter

To simplify the modelling of this system the following assumptions are assumed to be true:

- A1) the power grid is assumed to be predominantly inductive, modelled by a sinusoidal source V_d in series with an inductance L_{g2} with parasitic resistance R_{g2} ;
- A2) the input bus is assumed stabilised and represented by a DC source;
- A3) Filter output voltage and PCC voltage have guaranteed synchronism;
- A4) converter switches are considered ideal.

The electrical diagram of this system is shown in Figure 1. Note that the equivalent LCL circuit is represented by Thevenin equivalent in relation to the PCC. Also, R_c and L_c are the converter resistance and inductance, respectively. In addition, C is the capacitance of the LCL filter and $L_g = L_{g1} + L_{g2}$ and $R_g = R_{g1} + R_{g2}$, which are the total grid-side inductance and total grid-side resistance, respectively.

As the abc coordinate model is coupled [27], the control design becomes a complex task. Then, the abc coordinate model is transformed into its equivalent $\alpha\beta 0$ coordinates model, as shown in Figure 2. It results on two identical decoupled single-phase linear time-invariant (LIT) systems, which can be controlled independently. Note that, considering equilibrated phases, there is no path for current conduction on the 0 axis, and so it can be disregarded. The transformation

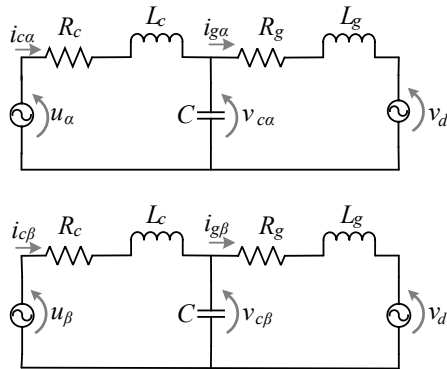


Fig. 2. Equivalent circuit of grid-tied voltage-fed 3-wire static converter with LCL filter in $\alpha\beta$ coordinates, with equilibrated phases

Clarke Transform, is shown below [39],

$$T_{\alpha\beta 0} = \frac{2}{3} \begin{bmatrix} 1 & -\frac{1}{2} & -\frac{1}{2} \\ 0 & \frac{\sqrt{3}}{2} & -\frac{\sqrt{3}}{2} \\ \frac{1}{2} & \frac{1}{2} & \frac{1}{2} \end{bmatrix}. \quad (1)$$

It is noteworthy that this transformation, with the term $2/3$, is known as the invariant transformation in voltage and current, since the magnitude of coordinate quantities $\alpha\beta 0$ is equal to their correspondent magnitude on abc coordinates.

For simplicity, consider only one single-phase circuit from Figure 2. The transfer function of decoupled single-phase LIT systems, with disconnected converter ($v_d = 0$), results

$$G(s) = \frac{i_g(s)}{u(s)} = \frac{1}{a_1 s^3 + a_2 s^2 + a_3 s + a_4}, \quad (2)$$

where $i_g(s)$ and $u(s)$ are the grid-side currents and the voltage synthesised by converter, respectively. Besides, $a_1 = L_g L_c C$, $a_2 = (R_g L_c + R_c L_g) C$, $a_3 = L_c + L_g + R_g R_c C$ and $a_4 = R_g + R_c$. Or yet,

$$G(s) = \frac{\frac{1}{L_g L_c C}}{s^3 + \frac{(R_g L_c + R_c L_g)}{L_g L_c} s^2 + \frac{(L_c + L_g + R_g R_c C)}{L_g L_c} s + \frac{R_g + R_c}{L_g L_c C}}. \quad (3)$$

A. Reduced System Model

The nominal plant parameters are presented in Table I. The filter was designed following the steps presented on [8]. It is noteworthy that parasitic resistance R_c and R_{g1} are only approximate values, since they vary on plant.

TABLE I
LCL Filter Parameters

Symbol	Parameter	Value
L_c	Converter-side inductance	1mH
R_c	Converter-side resistance	50mΩ
C	Capacitance of LCL filter	62μF
L_{g1}	Grid-side inductance	0.3mH
R_{g1}	Grid-side resistance	50mΩ

For the purpose of designing a reduced order adaptive controller, the plant was modelled as

$$G(s) = G_0(s) + \mu \Delta_a(s), \quad (4)$$

in α and β , where $G_0(s)$ is the part considered known, for reduced order controller design, and $\mu\Delta_a$ is an additive dynamics. The $G_0(s)$ part was modelled as a first order transfer function, obtained considering $C = 0$ in (2), which corresponds to the real pole of the continuous-time plant,

$$G_0(s) = \frac{1}{(L_c + L_g)s + R_c + R_g}. \quad (5)$$

Or yet,

$$G_0(s) = \frac{1}{s + \frac{R_c + R_g}{L_c + L_g}}. \quad (6)$$

By the other hand, the $\mu\Delta_a$ part corresponds to the pair of complex conjugate poles, considered as unmodelled dynamics from the point of controller's view. The $\mu\Delta_a$ dynamics is calculated by $G(s) - G_0(s)$. Then, subtracting (5) from (2), follows

$$\mu\Delta_a(s) = -C \frac{L_g L_c s^3 + (R_g L_c + R_c L_g) s^2 + R_g R_c s}{a_5 a_6}, \quad (7)$$

where $a_5 = L_g L_c C s^3 + (R_g L_c + R_c L_g) C s^2 + (L_c + L_g + R_g R_c C) s + R_g + R_c$ and $a_6 = (L_c + L_g) s + R_c + R_g$. From (7), it is clear that $\mu = C$, which is the main contribution for unmodelled dynamics. Therefore, a bigger capacitor, will imply on lower resonance frequency and consequently, more influential this dynamics will be on plant response. Then, to neglect the capacitor on LCL filter modelling, with objective of designing a reduced order controller, the LCL filter capacitance have to be $C \in [0, C^*)$, where C^* the maximum value of capacitance that can be considered as non-dominant dynamics in the response of the LCL filter. As, generally, on the LCL filter designs, the capacitor value is limited by the decrease of the power factor at rated power, commonly less than 5% [8], then, in these cases, this order reduction of the LCL filter model, can be applied for the purpose of designing robust adaptive controllers.

The Bode diagram, shown in Figure 3, shows the dynamics of the complete plant model, $G(s)$, the reduced plant model, $G_0(s)$, and additive dynamics, $\mu\Delta_a$.

III. DISCRETE-TIME ROBUST MODEL REFERENCE ADAPTIVE CONTROL

In this Section is presented the direct Discrete-Time RMRAC theory, design and experimental results. For RMRAC strategies, the plant is described as

$$G(z) = G_0(z)[1 + \mu\Delta_m(z)] + \mu\Delta_a(z), \quad (8)$$

where $\mu\Delta_m$ is the unmodelled multiplicative dynamics and the modelled part of the plant is described as

$$G_0(z) = k_p \frac{Z_p(z)}{R_p(z)}. \quad (9)$$

To be implementable, the plant is subject to following assumptions:

- P1) The signal of high gain k_p is known;
- P2) $Z_p(z)$ and $R_p(z)$ are monic polynomials of degree m and

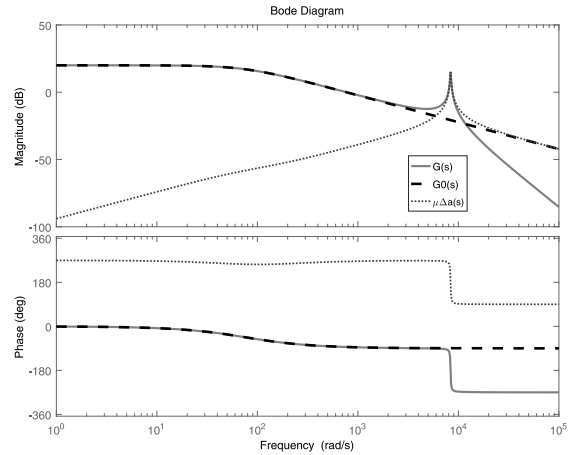


Fig. 3. Bode Diagram of LCL filter, reduced order model and additive dynamics

n , respectively;

P3) $Z_p(z)$ is a Schur polynomial;

P4) $\Delta_m(z)$ is a Schur transfer function;

P5) $\Delta_a(z)$ is a strictly proper Schur transfer function;

P6) The lower bound on stability margin of additive dynamics $\Delta_a(z)$ and multiplicative dynamics $\Delta_m(z)$ are known.

Relating the assumptions to the plant, we note that all assumptions are conformed or is satisfiable. For assumption P1, note that k_p of LCL model and its reduced order model, are known. Furthermore, by discrete-time transfer functions knowledge, the monic polynomials degrees are acquired, satisfying assumption P2. Besides, assumption P3 is also satisfied, once the polynomial $Z_p(z)$ is complete. Finally, assumptions P4 to P6 can be satisfiable depending on unmodelled dynamics, which the plant is subject. Note that, by approximating LCL filter to a first order transfer function in (5) and thus, the unmodelled dynamics are considered as (7), with identified LCL parameters satisfy assumptions P4 to P6, considering $\Delta_m = 0$. More details are presented next, on controller design.

The reference model is described as

$$W_m(z) = \frac{k_m}{R_m(z)}, \quad (10)$$

where k_m is the $W_m(z)$ high frequency gain. It has to satisfy the following assumption:

P7) $R_m(z)$ is an arbitrary Schur monic polynomial of relative degree $n^* = n - m > 0$. which is easily conformed, once the model reference is chosen by designer.

The structure of these controllers for SISO plants is well-discussed in [40]. The control action is determined from

$$\theta^T(k) \omega(k) + r(k) = 0, \quad (11)$$

where $r(k)$ is the reference signal, $\theta(k)$ is the adaptive gains vector and $\omega(k)$ are reconstructive filters, composed by $\omega_1(k)$ and $\omega_2(k)$, which have the following structure:

$$\begin{aligned} \omega_1(k+1) &= (\mathbf{I} + \mathbf{F}T_s) \omega_1(k) + \mathbf{q}u(k), \\ \omega_2(k+1) &= (\mathbf{I} + \mathbf{F}T_s) \omega_2(k) + \mathbf{q}y(k), \end{aligned} \quad (12)$$

where \mathbf{I} is an identity matrix of dimensions $n \times n$ and (\mathbf{F}, \mathbf{q}) is a controllable pair with a stable matrix \mathbf{F} and a controllable parameters vector \mathbf{q} , with dimension $n_p - 1 \times n_p - 1$ and $n_p - 1$, respectively [41]. This approach is known as input-output because filters reconstruct internal states of the plant, which will not necessarily be the plant states on space state.

The gain adaptation law is the Gradient algorithm, calculated as follows [40],

$$\boldsymbol{\theta}(k+1) = \boldsymbol{\theta}(k) - T_s \sigma(k) \boldsymbol{\Gamma} \boldsymbol{\theta}(k) - T_s \kappa \frac{\boldsymbol{\Gamma} \boldsymbol{\zeta}(k) \boldsymbol{\varepsilon}(k)}{m^2(k)}, \quad (13)$$

where the augmented error, $\boldsymbol{\varepsilon}(k)$, is

$$\boldsymbol{\varepsilon}(k) = e_1(k) + \boldsymbol{\theta}^T(k) \boldsymbol{\zeta}(k) - y_m(k), \quad (14)$$

and the auxiliary vector $\boldsymbol{\zeta}$ is

$$\boldsymbol{\zeta} = W_m(z) \boldsymbol{\omega}, \quad (15)$$

being $e_1(k)$ the tracking error, given by $e_1 = y(k) - y_m(k)$. Moreover, $\boldsymbol{\zeta}(k)$ is the vector $\boldsymbol{\omega}(k)$ filtered by reference model, $W_m(z)$. In addition, the majorant signal, used to ensure that all closed-loop signals are bounded, is given by

$$\bar{m}^2(k) = m^2(k) + \boldsymbol{\zeta}^T(k) \boldsymbol{\Gamma} \boldsymbol{\zeta}(k), \quad (16)$$

where

$$m(k+1) = (1 - T_s \delta_0) m(k) + T_s \delta_1 (1 + |u(k)| + |y(k)|), \quad (17)$$

being $m(0) > \delta_1 / \delta_0$ and $\delta_0 + \delta_1 \leq \min[p_0, q_0]$. Also, $\delta_1 > 0$ and $q_0 > 0$ such that poles of $W_m(z - q_0)$ and eigenvalues of $F + q_0 \mathbf{I}$ are stable, and $0 < p_0 < 1$ is the known lower bound on the stability margin of p , where p are the poles of $\Delta_m(z - p)$, $\Delta_a(z - p)$ are stable [41].

The $\boldsymbol{\Gamma}$ parameter is a symmetric positive matrix, with dimension $n \times n$, which defines the convergence rate of plant response relative to the reference model output. Since this parameter also compound the majorant signal $m^2(k)$, its range of choice is considerably large. However, to accelerate parametric convergence, a positive factor κ is used on (13). It is emphasised that majorant signal $m^2(k)$ can be modified according to the project's needs. Furthermore, it was also incorporated the σ -modification to the parameter adaptation algorithm, to increase its robustness and avoid parameters drifting [42]. This modification is given by

$$\sigma(k) = \begin{cases} 0 & \text{if } \|\boldsymbol{\theta}(k)\| < M_0 \\ \sigma_0 \left(\frac{\|\boldsymbol{\theta}(k)\|}{M_0} - 1 \right) & \text{if } M_0 \leq \|\boldsymbol{\theta}(k)\| < 2M_0, \\ \sigma_0 & \text{if } \|\boldsymbol{\theta}(k)\| \geq 2M_0 \end{cases} \quad (18)$$

where $M_0 > \|\boldsymbol{\theta}^*\|$ is the upper limit of $\boldsymbol{\theta}(k)$ norm, oversized due to lack of knowledge of $\|\boldsymbol{\theta}^*\|$ and σ_0 is the maximum value of the modification function. The block diagram of this control strategy is shown in Figure 4. Note that tracking error is calculated in relation to the model reference output, however, the reference signal is also used on control law. Besides, the control law and measure system output are filtered

and the resulting signals, with majorant signal and augmented error, are also used to the adaptive gains computation.

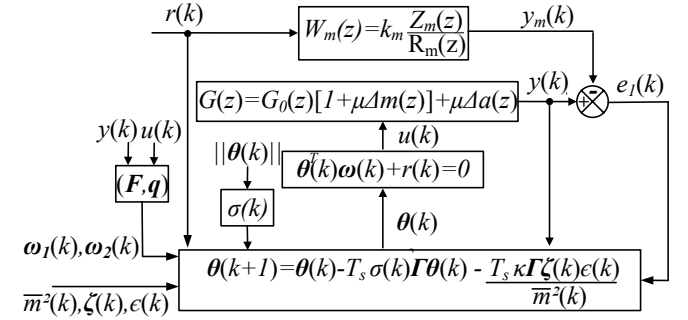


Fig. 4. Block diagram of high order RMRAC

As the grid-tied voltage-fed 3-wire static converter with LCL filter is a third order system, then $\boldsymbol{\omega}_1(k)$ and $\boldsymbol{\omega}_2(k)$ filters has dimension 2×2 . Thus, the vector $\boldsymbol{\omega}(k)$ is given by $\boldsymbol{\omega}(k) = [\boldsymbol{\omega}_{11}(k) \boldsymbol{\omega}_{12}(k) \boldsymbol{\omega}_{21}(k) \boldsymbol{\omega}_{22}(k) y(k) u(k) V_s(k) V_c(k)]^T$, where $V_s(k)$ and $V_c(k)$ are the phase and quadrature components of the exogenous disturbance, respectively. In this grid-tied application, the disturbance is the grid fundamental harmonic. Note that $u(k)$ is inside $\boldsymbol{\omega}(k)$ vector, and the implementable control law will present the $\theta_u(k)$ gain in the denominator. This is the only parameter that must be initialised with correct signal, to avoid division by zero.

The phase ($V_s(k)$) and quadrature ($V_c(k)$) components of the grid disturbance are described by $V_s(k) = A_s \sin(\omega_d k T_s + \phi_s)$ and $V_c(k) = A_c \cos(\omega_d k T_s + \phi_c)$, where A , ω_d and ϕ are amplitude, frequency and phase of $V_s(k)$ and $V_c(k)$ components, respectively. Note that $\boldsymbol{\theta}(k)$ vector is adjusted in function of respective dynamics that compounds the vector $\boldsymbol{\omega}(k)$, it means $\boldsymbol{\theta}(k) = [\theta_{11}(k) \theta_{12}(k) \theta_{21}(k) \theta_{22}(k) \theta_y(k) \theta_u(k) \theta_s(k) \theta_c(k)]^T$.

IV. DISCRETE-TIME REDUCED ORDER ROBUST MODEL REFERENCE ADAPTIVE CONTROL

In this Section is presented the proposed direct discrete-time reduced order RMRAC to the grid-side current control on a grid-tied voltage-fed 3-wire static converter with LCL filter.

The control action remains the same law shown in (11) and have to respect the same assumptions. However, as it considers the nominal part of the plant as a first order transfer function, then the $\boldsymbol{\omega}(k)$ is compound by a smaller set of parameters, given by $\boldsymbol{\omega}(k) = [u(k) y(k) V_s(k) V_c(k)]^T$, once, there no $\boldsymbol{\omega}_1$ and $\boldsymbol{\omega}_2$ to compute, therefore $\boldsymbol{\theta}(k)$ is $\boldsymbol{\theta}(k) = [\theta_u(k) \theta_y(k) \theta_s(k) \theta_c(k)]^T$.

The Gradient algorithm, used to parameters adaptation, is the same shown on (13),

$$\boldsymbol{\theta}(k+1) = \boldsymbol{\theta}(k) - T_s \sigma(k) \boldsymbol{\Gamma} \boldsymbol{\theta}(k) - T_s \kappa \frac{\boldsymbol{\Gamma} \boldsymbol{\zeta}(k) \boldsymbol{\varepsilon}(k)}{m^2(k)} \quad (19)$$

where the augmented error is

$$\boldsymbol{\varepsilon}(k) = e_1(k) + \boldsymbol{\theta}^T(k) \boldsymbol{\zeta}(k) - y_m(k) \quad (20)$$

and the auxiliary vector $\boldsymbol{\zeta}$ is

$$\boldsymbol{\zeta} = W_m(z) \boldsymbol{\omega} \quad (21)$$

The σ -modification also remains the same algorithm used on high order RMRAC, shown on (18), as well as the majorant signal $m(k)$, shown in (16). The block diagram of reduced order control strategy is shown below. Note that, as this control approach is of first order, it does not need filters for plant output and control action to adjust the gains. The other interactions are similar to the higher order RMRAC.

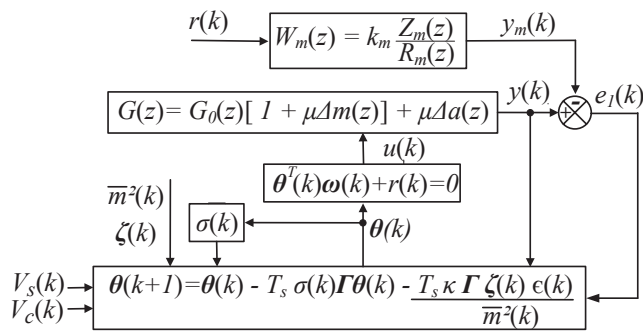


Fig. 5. Block diagram of reduced order RMRAC

V. EXPERIMENTAL RESULTS

Both control strategies were tested in a laboratory prototype, implemented on a DSP (Digital Signal Processor), a TMS320F28335 Delfino microcontroller from Texas Instruments. The prototype has the characteristics (L_C , C and L_{g1}) from Table I, whereas the parameters R_C and R_{g1} are unknown, as well as the parameters of the grid, R_{g2} and L_{g2} . The experimental setup is shown in Figure 6.

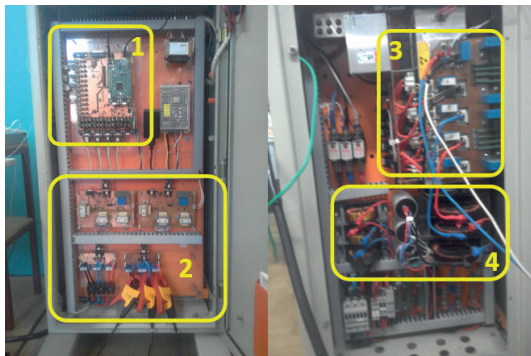


Fig. 6. Prototype: 1: DSP, 2: sensors, 3: Converter, 4: LCL filter

The line voltage range for all tests was 110V, adjusted by a three-phase transformer. In addition, the DC bus voltage has been set at 250V. This voltage is not controlled, however, it did not interfere in the control performance.

The converter's power is 5.4kW, its switching frequency and the controller's sampling frequency were both 5.040kHz, while the acquisition frequency of DSP was one quarter of it, that is, 1.260kHz (saves one sample every four controller interruptions), to capture sufficient data to evaluate the controller parameters convergence. This approach was necessary due to the DSP memory limitation. Therefore, as the DSP buffer saves 2000 samples, the time of each test was approximately 1.6s.

Also, to evaluate the controller performance, a 1mH inductance in series with the grid is triggered at a certain

moment of the test, opening the switch, causing a parametric variation over grid impedance. In this instant, the grid impedance is increased, by addition of 1mH inductance, turning the grid weaker. Figure 7 shows the scheme of this parametric variation test.

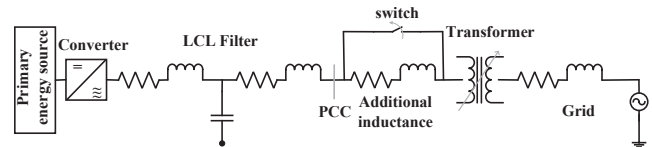


Fig. 7. Additional inductance in series with grid

It is also noteworthy that synchronisation of controller with the grid voltages was ensured with a Kalman Filter [43]. To do this, line voltages on PCC are measured, converted to phase voltages in abc coordinates and then converted to phase voltages in $\alpha\beta$. Following, these voltages are used to obtain the phase and quadrature signals of the grid fundamental components, which are used for disturbance rejection and current reference generation. Also, to synthesise the control law, a Space Vector Modulation was implemented [44].

A. High Order RMRAC

Firstly, note that when plant, shown on (3) with parameters of Table I, be discretised by Z transform, with a ZOH (Zero Order Hold) and implementation delay, a nonminimum phase zero will appear in $z = -3.0933$, as shown on $G(z)$. The other zero is localised in $z = -0.3163$,

$$G(z) = \frac{0.06033z^2 + 0.2057z + 0.05903}{z(z^3 - 0.8117z^2 + 0.8022z - 0.9579)}. \quad (22)$$

Then, to satisfy assumption P3, the nominal part of the plant, used to controller design, was modelled as

$$G_0(z) = \frac{0.32636z - 0.0013}{z(z^3 - 0.8117z^2 + 0.8022z - 0.9579)}, \quad (23)$$

which is a minimum phase model. Then, the additive dynamics is calculated as $\mu\Delta_a(z) = G(z) - G_0(z)$, which results in a transfer function with relative degree equal to 3, given by

$$\mu\Delta_a(z) = \frac{0.06033(z-1)^2}{z(z^3 - 0.8117z^2 + 0.8022z - 0.9579)}. \quad (24)$$

The controller parameters were defined as $\Gamma = 40I$, $\kappa = 1000$, $\sigma_0 = 0.1$, $M_0 = 10$, $\delta_0 = 0.7$ and $\delta_1 = 1$. Due to adaptive nature of the controller, the parameters design is flexible. It choose comes from robustness analysis, based on Lyapunov stability, here omitted. However, by experience, the parameters can be set as follows: $\Gamma\kappa T_s \leq 20$; δ_0 and δ_1 are chosen to act as a slow dynamics filter to smooth $\bar{m}(k)$ response; and M_0 can be securely oversized, as shown on [45], where $M_0 \geq 2\|\theta^*\|$. Besides, the reference model was designed with same relative degree of modelled part of plant ($G_0(z)$) and to have unit gain in steady state,

$$W_m(z) = \frac{0.343}{(z-0.3)^3}. \quad (25)$$

The initial gains $\theta(0)$, in $\alpha\beta$, were defined as

$$\theta_{\alpha}(0) = \begin{bmatrix} -2.3075082 \\ 0 \\ -0.65603852 \\ 0 \\ -1.0379406 \\ -1.9491602 \\ 3.3076313 \\ -0.36709696 \end{bmatrix}, \quad \theta_{\beta}(0) = \begin{bmatrix} -0.84257501 \\ 0 \\ -0.32428530 \\ 0 \\ -0.83423382 \\ -1.2983845 \\ 1.5830313 \\ -0.11256287 \end{bmatrix}.$$

These gains were set by choosing final gains of a simulation, used to be initialised closer to θ^* and avoid excessive overshoot in the initial transient.

The reference signal is extracted from the grid through Kalman filter and then normalised [43]. The initial reference signal has amplitude of 20A and it is increased to 30A when time reaches 0.4s. At 0.8s, a parametric variation is imposed on the grid impedance by closing the switch that adds 1mH in series with the electrical grid. This procedure was adopted for all tests. Figure 8 shows the tracking errors given between y_m and y and the control actions are presented on Figure 9. Next, the gains adaptation are shown in Figure 10 and 11, in α and β , respectively.

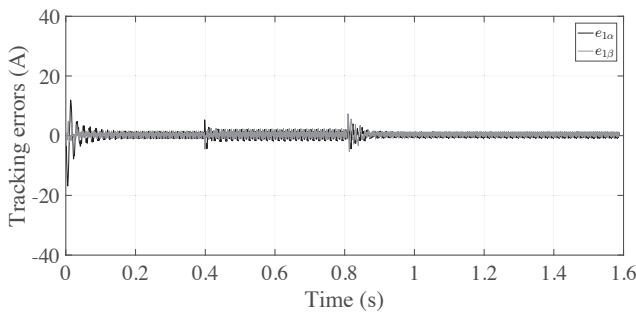


Fig. 8. Tracking errors in $\alpha\beta$

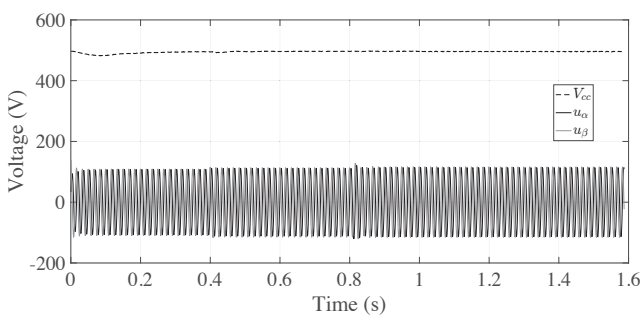


Fig. 9. Control actions in $\alpha\beta$ and V_{cc}

As can be seen on Figure 8, the tracking errors tend to a small value quickly. Due to gains initialisation closer to θ^* , the initial transient regime was short and as expected the excessive overshoot was avoided, not exceeding 3.09A. Moreover, after gains converged to a set of bounded values, the tracking errors remains small, even when the reference amplitude is increased and the grid inductance is varied. In addition, the V_{cc} is presented with control actions, where is

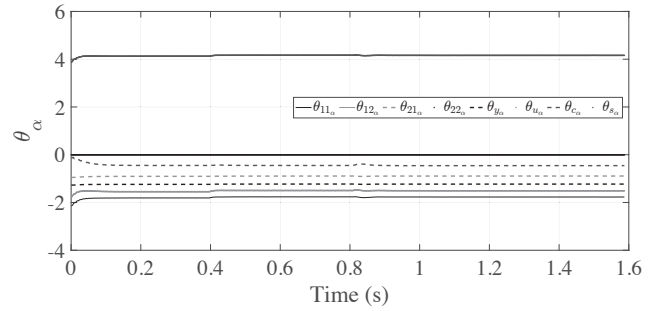


Fig. 10. Gains adaptation in α

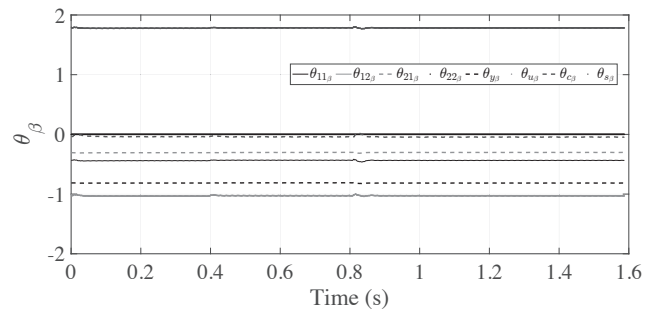


Fig. 11. Gains adaptation in β

possible to note a small sag on voltage source, once it is not controlled. However, the controller stability was not affected by it. Besides, the control actions did not required excessive voltage to deal with parametric variations and exogenous disturbance rejection, keeping the grid-side currents tracking, as shown on Figure 9. For a better analysis of controller performance, from Figure 12 to Figure 14, it is shown the following events: reference change instant, parametric variation instant and steady state regime, respectively.

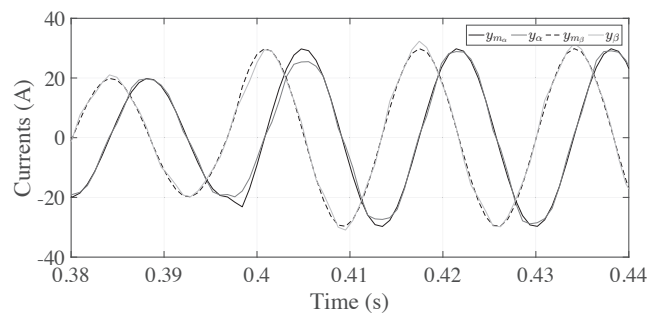


Fig. 12. Grid-side currents in $\alpha\beta$, on reference change transient

In Figure 12, it can be observed the fast current tracking, when reference signal has its amplitude increased from 20A to 30A. It takes around 30ms to reach model reference output, in both coordinates and the overshoot did not exceed 2.31A. Furthermore, in the Figure 13, the controller robustness to parametric variations can be observed, once at 0.8s the grid inductance is increased by 1mH. Note that this transient takes around 40ms to be overcome and again an overshoot is observed, with almost 3.6A. Finally, in steady-state, the

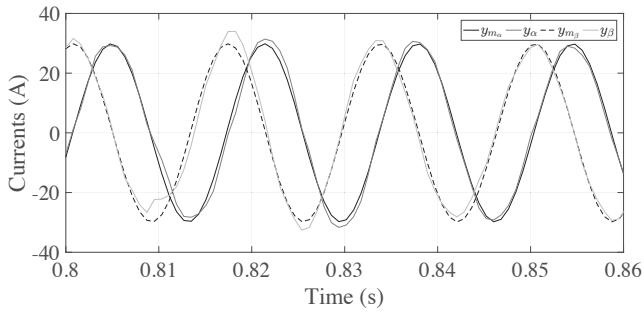


Fig. 13. Grid-side currents in $\alpha\beta$, on parametric variation transient

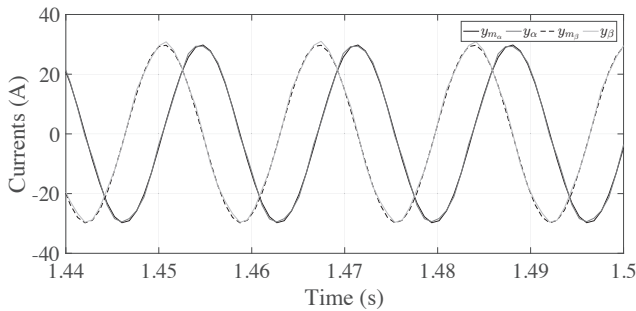


Fig. 14. Grid-side currents tracking in $\alpha\beta$, on steady state regime

model reference output is tracked very closely, as can be seen on Figure 14, where the currents on α and β are almost overlapped to their respective model reference output. In addition, on Figure 15, the grid-side currents in steady state, acquired from oscilloscope, are presented. Next, on Figure 16, the 50 first harmonic contents are presented.

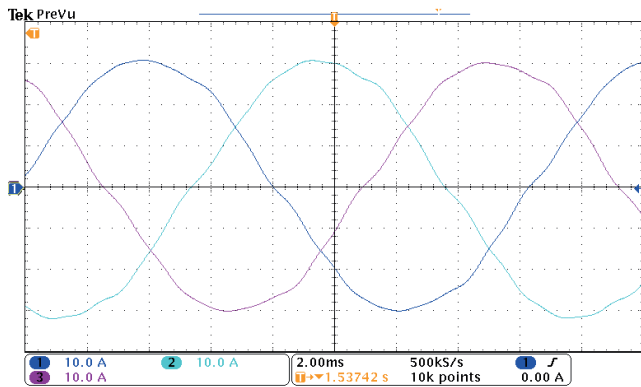


Fig. 15. Grid-side currents in abc , on steady state regime, acquired from oscilloscope

The total harmonics distortion was 2.48151% and all harmonic contents, even and odd, respected the IEEE 1547 Standard. It reinforces the discussion of $\alpha\beta$ currents control performance by RMRAC, and its potentiality of application. Hereupon, in the next subsection, it is presented an equivalent controller in means of performance, however with low computational burden, to be implementable in a larger family of microcontrollers, which deal with more restrict memory issues and to reduce controller design complexity.

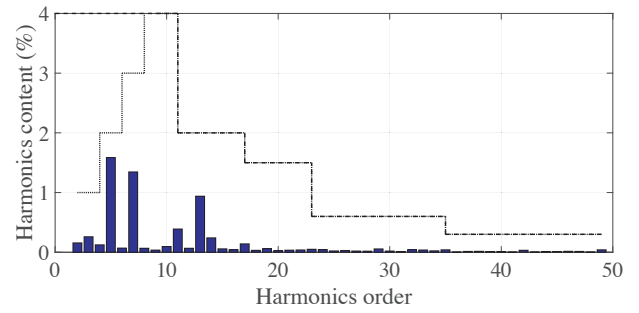


Fig. 16. Harmonic contents, where the dashed line represents the upper limits for odd harmonics and the dotted line represents the upper limits for even harmonics, as described by IEEE 1547 Standard

B. Reduced Order RMRAC

For proposed reduced order control method, consider $G_0(s)$ as (6). By application of Z transform, with a ZOH (Zero Order Hold), it is obtained the discrete-time transfer function, $G_0(z)$, which has only a minimum-phase zero,

$$G_0(z) = \frac{0.1515}{z - 0.9849}. \quad (26)$$

The experimental tests follows the same steps previously discussed in the previous subsection. The controller parameters were set as $\Gamma = 200I$, $\kappa = 1000$, $\sigma_0 = 0.1$, $M_0 = 5$, $\delta_0 = 0.7$ and $\delta_1 = 1$, following the same design approach used for higher order RMRAC. The reference model is

$$W_m(z) = \frac{0.7}{z - 0.3}, \quad (27)$$

and the initial gains $\theta(0)$, in $\alpha\beta$, were defined as:

$$\theta_\alpha(0) = \begin{bmatrix} -1.1132272 \\ -1.7000784 \\ 1.2114146 \\ 0.1714769 \end{bmatrix}, \quad \theta_\beta(0) = \begin{bmatrix} -1.1196474 \\ -0.0706902 \\ 0.9791124 \\ 0.0862891 \end{bmatrix}.$$

Figure 17 presents the tracking errors, in $\alpha\beta$ and control actions, besides V_{cc} , are shown on Figure 18. Next, the gains adaptation, in α and β , are presented in Figure 19 and Figure 20, respectively.

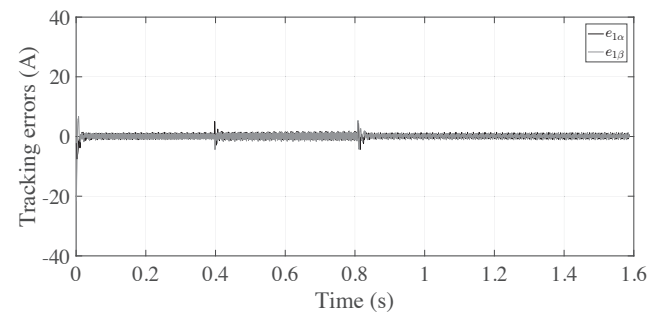


Fig. 17. Tracking errors in $\alpha\beta$

Note, on Figure 17, that tracking error converge fast for small values, as well as the conventional high order RMRAC.

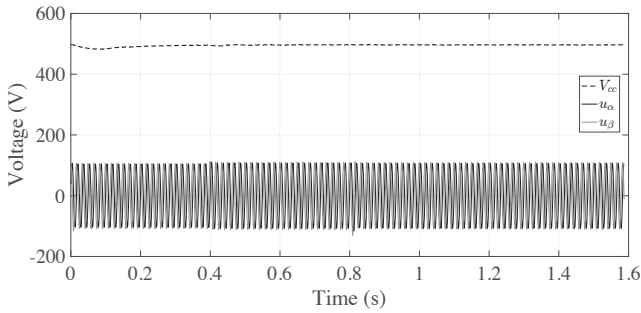


Fig. 18. Control actions in $\alpha\beta$ and V_{cc}

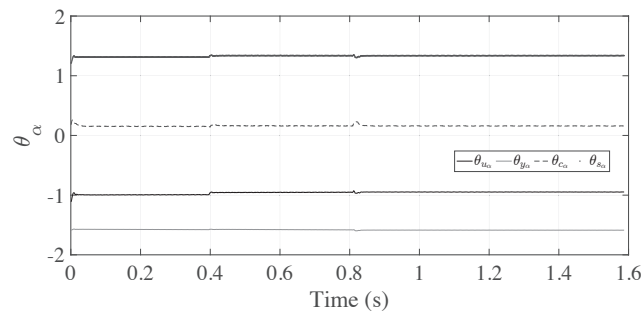


Fig. 19. Gains adaptation in α

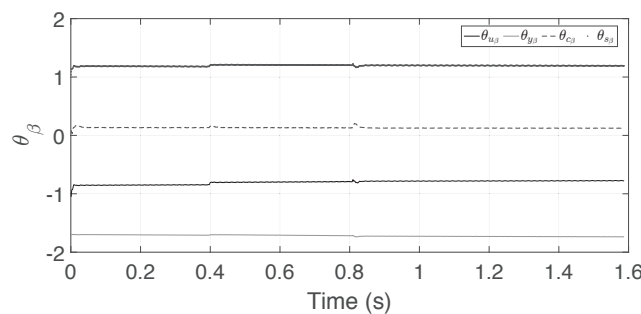


Fig. 20. Gains adaptation in β

It only does not reach zero error due to converter switching dynamics. Moreover, only a small overshoot occurred on initial transient regime, not exceeding 1.63A. Furthermore, no additional effort was required from control action, as can be observed by comparison of Figure 18 (reduced order RMRAC control action) and Figure 9 (conventional high order RMRAC control action), under same conditions. Besides, the auto adjustable control parameters adapts as fast as high order RMRAC to compensate unmodelled dynamics influence.

As was discussed for previously presented controller, from Figure 21 to Figure 23 following events are shown: reference change instant, parametric variation instant and steady state regime, respectively.

Note that proposed reduced order RMRAC can deal properly with exogenous disturbances and parametric variations as well as the high order RMRAC, keeping a satisfactory grid-side current tracking and transient response, with relevant computational burden reduction. From Figure

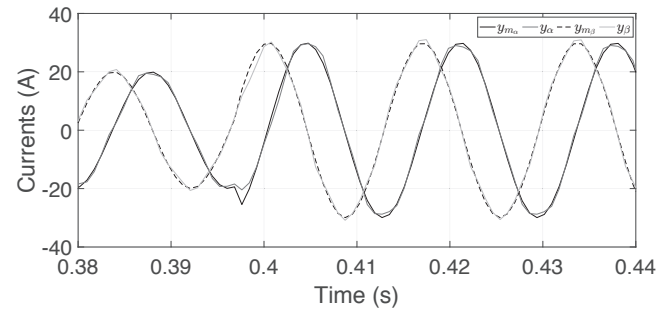


Fig. 21. Grid-side currents in $\alpha\beta$, on reference change transient

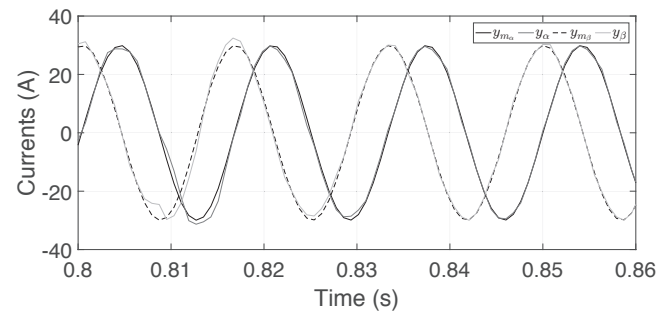


Fig. 22. Grid-side currents in $\alpha\beta$, on parametric variation transient

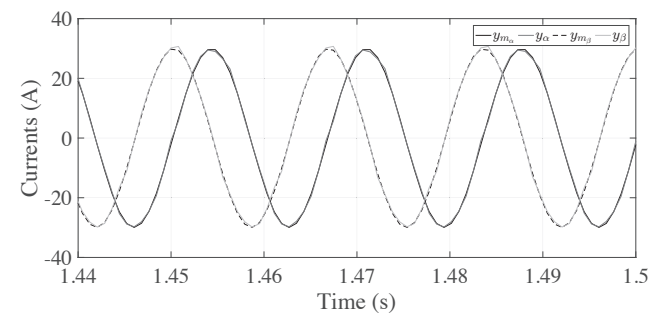


Fig. 23. Grid-side currents tracking in $\alpha\beta$, on steady state regime

21, it can be observed that currents tracking takes around 15ms to be very close to model reference output and the overshoot did not exceed 1.04A. Also, when grid inductance is varied, the controller fast readapts their gains to maintain currents tracking, achieved in less than 20ms and with overshoot not exceeding 2.45A. In addition, in steady state, shown on Fig 23, the grid-side currents, in α and β , are tracking very closely their respective reference signals.

To reinforce $\alpha\beta$ currents control, the grid-injected currents on steady state regime, acquired from oscilloscope, are shown on Figure 24. Furthermore, the 50 first harmonic contents are presented on Figure 25.

As expected, once $\alpha\beta$ currents were properly controlled, the grid-injected currents, in abc , acquired from oscilloscope, presented satisfactory quality. The total harmonics distortion with the reduced order control approach was 2.47365%, similar to high order RMRAC. Also, all harmonic contents of grid-side currents respected the IEEE 1547 Standard,

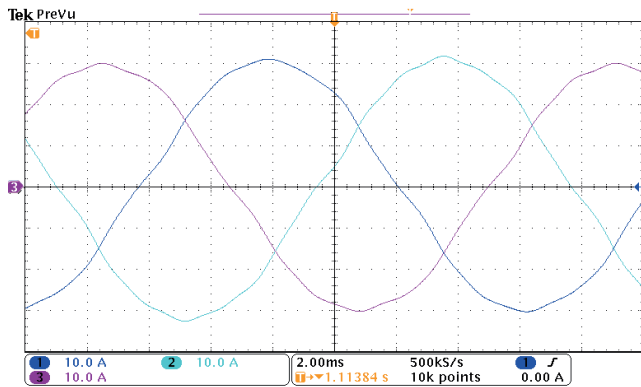


Fig. 24. Grid-side currents in *abc*, on steady state regime, acquired from oscilloscope

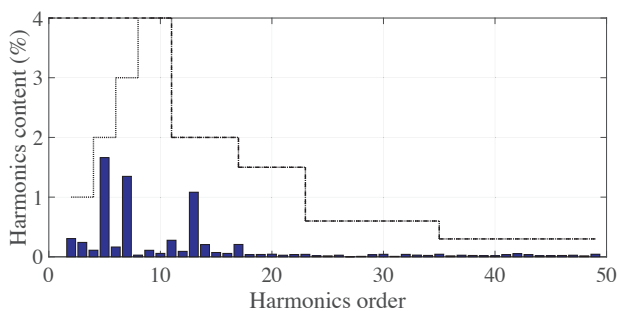


Fig. 25. Harmonic contents, where the dashed line represents the upper limits for odd harmonics and the dotted line represents the upper limits for even harmonics, as described by IEEE 1547 Standard

reinforcing the potential applicability of proposed control method. For grid-tied power converters connected to the grid by LCL filters, this controller keeps good-quality of grid-injected currents and saves computational burden for other parallel microcontroller activities or allowing apply a robust adaptive control in more memory-restricted microcontroller.

To compare briefly the computational burden of the high order RMRAC, discussed in the previous section, and the proposed reduced order RMRAC applied to grid-tied converter by LCL filter, note the quantity of calculations involved in both control strategy: the high order RMRAC requires 628 operations (182 addition/subtraction and 446 multiplication/division), which requires $37.56\mu s$ to execute it, while the reduced order RMRAC requires only 222 operations (60 addition/subtraction and 162 multiplication/division), which requires $15.39\mu s$. It means that reduced order controller requires approximately 65% less operations, which reflects in a 59% less time processing, than high order RMRAC, which alleviates significantly microcontroller requirements, besides has a simpler design.

VI. CONCLUSION

In this work, it was presented the design of a direct discrete-time reduced order Robust Model Reference Adaptive Control applied to the grid-side current control of a grid-tied voltage-fed 3-wire static converter with LCL filter. Firstly, the LCL model was reduced to a first order transfer function, by negligence of capacitor dynamics, approximating it to the L

filter model. Next, it was mathematically shown that additive dynamics is mainly influenced by neglected capacitors. The proposed control approach was designed using the reduced order LCL filter and compared with a high order RMRAC, conventionally applied on grid-tied converters with LCL filter. In general, both controllers results on currents control performance very similar, keeping robustness to parametric variation and exogenous disturbances, besides fast current tracking and parameters convergence. However, the proposed controller has as main advantage its simplicity. Due to it, less parameters have to be adapted, which reduces computational burden and turns easier its design and implementation, which is a great advantage for experimental implementation, mainly if microcontroller has low memory. Besides, experimental results performed in a DSP, a TMS320F28335 Delfino microcontroller, were presented to corroborate the control strategy and shown a satisfactory performance, with THD and harmonic contents respecting the IEEE 1547 Standard, even in the face of grid uncertainties, parametric variations of grid inductance and exogenous disturbances. Furthermore, the time processing of proposed control approach is 59% smaller than high order RMRAC. Thus, the proposed reduced order direct discrete-time RMRAC shown a potential controller for grid-tied power converters.

ACKNOWLEDGEMENTS

This study was financed in part by the Coordenação de Aperfeiçoamento de Pessoal de Nível Superior - Brasil (CAPES/PROEX)-Finance code 001. The authors would also like to thank the INCT-GD and the finance agencies (CNPq 465640/2014-1, CNPq Projeto 424997/2016-9, CAPES 23038.000776/2017-54 and FAPERGS 17/2551-0000517-1).

REFERENCES

- [1] M. Liserre, T. Sauter, J. Y. Hung, "Future energy systems: Integrating renewable energy sources into the smart power grid through industrial electronics", *IEEE Industrial Electronics Magazine*, vol. 4, no. 1, pp. 18–37, March 2010.
- [2] T. Kåberger, "Progress of renewable electricity replacing fossil fuels", *Global Energy Interconnection*, vol. 1, no. 1, pp. 48–52, January 2018.
- [3] R. Moradpour, H. Ardi, A. Tavakoli, "Design and implementation of a new SEPIC-based high step-up DC/DC converter for renewable energy applications", *IEEE Transactions on Industrial Electronics*, vol. 65, no. 2, pp. 1290–1297, July 2017.
- [4] B. Gu, J. Dominic, J.-S. Lai, C.-L. Chen, T. LaBella, B. Chen, "High reliability and efficiency single-phase transformerless inverter for grid-connected photovoltaic systems", *IEEE Transactions on Power Electronics*, vol. 28, no. 5, pp. 2235–2245, August 2012.
- [5] P. S. N. Filho, T. A. d. S. Barros, M. G. Villalva, E. R. Filho, "Modelagem Precisa para Análise e Projeto de Controle do Elo CC do Conversor Fonte de Tensão Trifásico com Filtro LCL Conectado à Rede Elétrica", *Eletrônica de Potência*, vol. 22, no. 1, pp. 7–18, Março 2017.

- [6] E. Twining, D. G. Holmes, “Grid current regulation of a three-phase voltage source inverter with an LCL input filter”, *IEEE Transactions on Power Electronics*, vol. 18, no. 3, pp. 888–895, May 2003.
- [7] R. Teodorescu, M. Liserre, P. Rodríguez, *Grid Converters for Photovoltaic and Wind Power Systems*, Wiley & Sons – IEEE, 2011.
- [8] M. Liserre, F. Blaabjerg, S. Hansen, “Design and control of an LCL-filter-based three-phase active rectifier”, *IEEE Transactions on Industry Applications*, vol. 41, no. 5, pp. 1281–1291, September 2005.
- [9] R. V. Tambara, J. M. Kanieski, J. R. Massing, M. Stefanello, H. A. Gründling, “A Discrete-Time Robust Adaptive Controller Applied to Grid-Connected Converters with LCL Filter”, *Journal of Control, Automation and Electrical Systems*, vol. 28, no. 3, pp. 371–379, 2017.
- [10] J. Dannehl, F. W. Fuchs, P. B. Thogersen, “PI state space current control of grid-connected PWM converters with LCL filters”, *IEEE Transactions on Power Electronics*, vol. 25, no. 9, pp. 2320–2330, April 2010.
- [11] G. Shen, D. Xu, L. Cao, X. Zhu, “An improved control strategy for grid-connected voltage source inverters with an LCL filter”, *IEEE Transactions on Power Electronics*, vol. 23, no. 4, pp. 1899–1906, July 2008.
- [12] M. Liserre, R. Teodorescu, F. Blaabjerg, “Stability of photovoltaic and wind turbine grid-connected inverters for a large set of grid impedance values”, *IEEE Transactions on Power Electronics*, vol. 21, no. 1, pp. 263–272, 2006.
- [13] R. Pena-Alzola, M. Liserre, F. Blaabjerg, R. Sebastián, J. Dannehl, F. W. Fuchs, “Analysis of the passive damping losses in LCL-filter-based grid converters”, *IEEE Transactions on Power Electronics*, vol. 28, no. 6, pp. 2642–2646, October 2012.
- [14] J. Dannehl, C. Wessels, F. W. Fuchs, “Limitations of voltage-oriented PI current control of grid-connected PWM rectifiers with LCL filters”, *IEEE Transactions on Industrial Electronics*, vol. 56, no. 2, pp. 380–388, November 2008.
- [15] M. B. Saïd-Romdhane, M. W. Naouar, I. Slama-Belkhdja, E. Monmasson, “Robust active damping methods for LCL filter-based grid-connected converters”, *IEEE Transactions on Power Electronics*, vol. 32, no. 9, pp. 6739–6750, November 2016.
- [16] G. Shen, X. Zhu, J. Zhang, D. Xu, “A new feedback method for PR current control of LCL-filter-based grid-connected inverter”, *IEEE Transactions on Industrial Electronics*, vol. 57, no. 6, pp. 2033–2041, February 2010.
- [17] Y. Jia, J. Zhao, X. Fu, “Direct grid current control of LCL-filtered grid-connected inverter mitigating grid voltage disturbance”, *IEEE Transactions on Power Electronics*, vol. 29, no. 3, pp. 1532–1541, May 2013.
- [18] L. A. Maccari, C. L. do Amaral Santini, H. Pinheiro, R. C. de Oliveira, V. F. Montagner, “Robust optimal current control for grid-connected three-phase pulse-width modulated converters”, *IET Power Electronics*, vol. 8, no. 8, pp. 1490–1499, 2015.
- [19] S. A. Khajehoddin, M. Karimi-Ghartemani, M. Ebrahimi, “Optimal and systematic design of current controller for grid-connected inverters”, *IEEE Journal of Emerging and Selected Topics in Power Electronics*, vol. 6, no. 2, pp. 812–824, August 2017.
- [20] I. J. Gabe, V. F. Montagner, H. Pinheiro, “Design and implementation of a robust current controller for VSI connected to the grid through an LCL filter”, *IEEE Transactions on Power Electronics*, vol. 24, no. 6, pp. 1444–1452, May 2009.
- [21] L. A. Maccari, J. R. Massing, L. Schuch, C. Rech, H. Pinheiro, R. C. Oliveira, V. F. Montagner, “LMI-based control for grid-connected converters with LCL filters under uncertain parameters”, *IEEE Transactions on Power Electronics*, vol. 29, no. 7, pp. 3776–3785, August 2013.
- [22] R. Guzman, L. G. de Vicuña, J. Morales, M. Castilla, J. Miret, “Model-based active damping control for three-phase voltage source inverters with LCL filter”, *IEEE Transactions on Power Electronics*, vol. 32, no. 7, pp. 5637–5650, September 2016.
- [23] G. G. Koch, L. A. Maccari, R. C. L. F. Oliveira, V. F. Montagner, “Robust \mathcal{H}_∞ State Feedback Controllers Based on Linear Matrix Inequalities Applied to Grid-Connected Converters”, *IEEE Transactions on Industrial Electronics*, vol. 66, no. 8, pp. 6021–6031, September 2019.
- [24] L. T. Martins, M. Stefanello, H. Pinheiro, R. P. Vieira, “Current Control of Grid-Tied LCL-VSI with a Sliding Mode Controller in a Multiloop Approach”, *IEEE Transactions on Power Electronics*, vol. 34, no. 12, pp. 12356–12367, March 2019.
- [25] R. Guzman, L. G. de Vicuña, M. Castilla, J. Miret, H. Martin, “Variable structure control in natural frame for three-phase grid-connected inverters with LCL filter”, *IEEE Transactions on Power Electronics*, vol. 33, no. 5, pp. 4512–4522, July 2017.
- [26] N. Panten, N. Hoffmann, F. W. Fuchs, “Finite control set model predictive current control for grid-connected voltage-source converters with LCL filters: A study based on different state feedbacks”, *IEEE Transactions on Power Electronics*, vol. 31, no. 7, pp. 5189–5200, September 2015.
- [27] J. R. Massing, M. Stefanello, H. A. Gründling, H. Pinheiro, “Adaptive current control for grid-connected converters with LCL filter”, *IEEE Transactions on Industrial Electronics*, vol. 59, no. 12, pp. 4681–4693, 2012.
- [28] J. M. Espi, J. Castello, R. Garcia-Gil, G. Garcera, E. Figueres, “An adaptive robust predictive current control for three-phase grid-connected inverters”, *IEEE Transactions on Industrial Electronics*, vol. 58, no. 8, pp. 3537–3546, October 2010.
- [29] R. V. Tambara, J. R. Massing, H. Pinheiro, H. A. Gründling, “A digital RMRAC controller based on a modified RLS algorithm applied to the control of the output currents of an LCL-filter connected to the grid”, in *2013 15th European Conference on Power Electronics and Applications (EPE)*, pp. 1–8, IEEE, 2013.

- [30] M. H. Durgante, H. F. B. Plotzki, M. Stefanello, “Combined active damping with adaptive current control for converters with LCL filters”, in *IECON 2013-39th Annual Conference of the IEEE Industrial Electronics Society*, pp. 520–525, IEEE, 2013.
- [31] M. Stefanello, J. R. Massing, R. P. Vieira, “Robust control of a grid-connected converter with an lcl-filter using a combined sliding mode and adaptive controller in a multi-loop framework”, in *IECON 2015-41st Annual Conference of the IEEE Industrial Electronics Society*, pp. 003726–003731, IEEE, January 2015.
- [32] C. He, J. Zhao, S. Zhang, K. Qu, “Adaptive current control strategy based on system sensitivity for grid-connected LCL-filter inverter in weak grid”, in *2016 IEEE Innovative Smart Grid Technologies-Asia (ISGT-Asia)*, pp. 418–423, IEEE, 2016.
- [33] R. V. Tambara, L. G. Scherer, H. A. Gründling, “A discrete-time MRAC-SM applied to grid connected converters with LCL-filter”, in *2018 IEEE 19th Workshop on Control and Modeling for Power Electronics (COMPEL)*, pp. 1–6, IEEE, September 2018.
- [34] A. Benrabah, F. Khoucha, K. Marouani, A. Kheloui, A. Raza, D. Xu, “Improved Grid-Side Current Control of LCL-Filtered Grid-Tied Inverters Under Weak Grid Conditions”, in *2019 Algerian Large Electrical Network Conference (CAGRE)*, pp. 1–5, IEEE, 2019.
- [35] K. J. Åström, P. Hagander, J. Sternby, “Zeros of sampled systems”, *Automatica*, vol. 20, no. 1, pp. 31–38, February 1984.
- [36] H. Elliott, “Direct adaptive pole placement with application to nonminimum phase system”, *IEEE Transactions on Automatic Control*, vol. 27, no. 3, pp. 720–722, June 1982.
- [37] D. Janecki, “Direct adaptive pole placement for plants having purely deterministic disturbances”, *IEEE Transactions on Automatic Control*, vol. 32, no. 3, pp. 187–189, February 1987.
- [38] J. H. Kim, K. K. Choi, “Direct adaptive control with integral action for nonminimum phase systems”, *IEEE Transactions on Automatic Control*, vol. 32, no. 5, pp. 438–442, May 1987.
- [39] W. Duesterhoeft, M. W. Schulz, E. Clarke, “Determination of instantaneous currents and voltages by means of alpha, beta, and zero components”, *Transactions of the American Institute of Electrical Engineers*, vol. 70, no. 2, pp. 1248–1255, July 1951.
- [40] P. A. Ioannou, J. Sun, *Robust adaptive control*, Courier Corporation, 2012.
- [41] P. Ioannou, K. Tsakalis, “A robust direct adaptive controller”, *IEEE Transactions on Automatic Control*, vol. 31, no. 11, pp. 1033–1043, November 1986.
- [42] R. Lozano, J. Collado, S. Mondie, “Model reference robust adaptive control without a priori knowledge of the high frequency gain”, *IEEE Transactions on Automatic Control*, vol. 35, no. 1, pp. 71–78, June 1990.
- [43] R. Cardoso, R. F. de Camargo, H. Pinheiro, H. A. Gründling, “Kalman filter based synchronisation methods”, *IET Generation, Transmission & Distribution*, vol. 2, no. 4, pp. 542–555, June 2008.
- [44] L. Michels, R. De Camargo, F. Botteron, H. Gründling, H. Pinheiro, “Generalised design methodology of second-order filters for voltage-source inverters with space-vector modulation”, *IEE Proceedings-Electric Power Applications*, vol. 153, no. 2, pp. 219–226, March 2006.
- [45] P. Ioannou, K. Tsakalis, “A robust discrete-time adaptive controller”, in *1986 25th IEEE Conference on Decision and Control*, pp. 838–843, IEEE, 1986.

BIOGRAPHIES

Paulo Jefferson Dias de Oliveira Ewald, received the B.Sc. in Automation Engineering and M. Sc. in Computer Engineering by Federal University of Rio Grande at (FURG), in 2016 and 2018, respectively. He worked as Auxiliary Professor at Federal University of Rio Grande, from 2017 to 2019. Currently, he is Ph.D. candidate in Electrical Engineer at Federal University of Santa Maria (UFSM) and Assistant Professor at Franciscan University (UFN). Besides, he is a researcher at the Power and Control Electronics Group (GEPOC). Also, he is a effective member of the Brazilian Society of Power Electronics (SOBRAEP). Your main research interests include adaptive control theory, renewable energy and power electronics control applications.

Rodrigo Varela Tambara, received the degree of Technician in Electrotechnics by Industrial Technical College of Santa Maria (CTISM) in 2004, B.Sc., M.Sc. and Ph.D. in Electrical Engineer by UFSM in 2008, 2010 and 2014, respectively. He worked as Assistant Professor at University Franciscan Centre (UNIFRA), from 2014 to 2016, and also worked as Adjunct Professor at UFSM, from 2016 to 2018. Currently, he is currently Adjunct Professor at CTISM and Substitute Coordinator of the higher course in Technology in Industrial Electronics. Besides, he is a researcher at GEPOC and at the Research and Development Group on Electrical and Computer Systems (GSEC). Also, he is a member of SOBRAEP. Your main research interests include control applications, electronic instrumentation and power electronics.

Hilton Abílio Gründling, received the B.Sc. in Electronics Engineering by Pontifical University of Rio Grande do Sul (PUCRS) in 1977, M. Sc. in Electrical Engineering from Federal University of Santa Catarina (UFSC) in 1980 and Ph.D. in Electronic and Computer Engineering by Technological Institute of Aeronautics (ITA) in 1995. He worked as Titular Professor at UFSM, from 1980 to 2016. Since 2017, he is Full Professor at UFSM Campus Cachoeira do Sul (UFSM-CS). Besides, he is a researcher at GEPOC. Your main research interests include electronic automation of electrical and industrial processes, acting mainly on discrete-time robust adaptive controllers and energy efficiency.